Theoretical Predictions of ^{31}P NMR Chemical Shift Threshold of Trimethylphosphine Oxide Absorbed on Solid Acid Catalysts

Anmin Zheng,[†,‡] Hailu Zhang,[†] Xin Lu,[§] Shang-Bin Liu,*[,‡] and Feng Deng*[,†]

State Key Laboratory of Magnetic Resonance and Atomic and Molecular Physics, Wuhan Center for Magnetic Resonance, Wuhan Institute of Physics and Mathematics, The Chinese Academy of Sciences, Wuhan 430071, China, Institute of Atomic and Molecular Sciences, Academia Sinica, P.O. Box 23-166, Taipei 106, Taiwan, and State Key Laboratory of Physical Chemistry of Solid Surface & Center for Theoretical Chemistry, College of Chemistry and Chemical Engineering, Xiamen University, Xiamen 361005, China

Received: October 9, 2007; In Final Form: January 25, 2008

The ^{31}P NMR chemical shifts of adsorbed trimethylphosphine oxide (TMPO) and the configurations of the corresponding $TMPOH^+$ complexes on Brønsted acid sites with varying acid strengths in modeled zeolites have been predicted theoretically by means of density functional theory (DFT) quantum chemical calculations. The configuration of each $TMPOH^+$ complex was optimized at the PW91/DNP level based on an 8T cluster model, whereas the ^{31}P chemical shifts were calculated with the gauge including atomic orbital (GIAO) approach at both the HF/TZVP and MP2/TZVP levels. A linear correlation between the ^{31}P chemical shift of adsorbed TMPO and the proton affinity of the solid acids was observed, and a threshold for superacidity (86 ppm) was determined. This threshold for superacidity was also confirmed by comparative investigations on other superacid systems, such as carborane acid and heteropolyoxometalate $H_3PW_{12}O_{40}$. In conjunction with the strong correlation between the MP2 and the HF ^{31}P isotropic shifts, the 8T cluster model was extended to more sophisticated models (up to 72T) that are not readily tractable at the GIAO-MP2 level, and a ^{31}P chemical shift of 86 ppm was determined for TMPO adsorbed on zeolite H-ZSM-5, which is in good agreement with the NMR experimental data.

1. Introduction

The acidic properties (such as type, strength, and distribution of acid sites) of solid acid catalysts have been extensively studied experimentally.[1−4] One of the crucial issues involved in the study of solid acid catalysts is the accurate determination of acid strength. Several spectroscopic and analytical methods such as IR spectroscopy, temperature-programmed desorption (TPD), and microcalorimetry have been employed to characterize the acidity of solid acid catalysts. In the more conventional NH_3 TPD and pyridine IR experiments, the ammonia and pyridine probe molecules are normally too basic to distinguish the subtle differences in acid distributions of solid acid catalysts; thus, only an average acid strength can be obtained. In this context, hydrogen-bonded bases (such as acetonitrile) might serve as preferential probes, as suggested by Gorte et al.[3,4] For example, the authors reported that the heats of adsorption for ammonia on Brønsted acid sites associated with framework Al and Fe species were nearly identical (35.9 kcal/mol) for H-[Al]-ZSM-5 and H-[Fe]-ZSM-5 zeolites, even though their catalytic activities during hydrocarbon reactions were dramatically different. On the other hand, the heats of adsorption observed for acetonitrile adsorbed on H-[Fe]-ZSM-5 and H-[Al]-ZSM-5 were 22.7 and 26.3 kcal/mol, respectively. In addition to the TPD and microcalorimetry methods, a variety of techniques have been developed recently for acidity characterization utilizing solid-state magic-angle-spinning (MAS) NMR spectroscopy of various probe molecules.[5−10] Although ^{1}H MAS NMR spectroscopy is capable of providing structural information about various hydroxyl groups on solid acid catalysts directly (including bridging OH groups; i.e., Brønsted acid site), it is limited by spectral resolution because of the narrow chemical shift range (ca. 20 ppm) available for the ^{1}H nucleus. As such, acid characterization by solid-state MAS NMR spectroscopy normally requires the adsorption of suitable probe molecules, such that valuable acid features (such as type, strength, and distribution of acid sites) as well as the interactions between the probe molecule and the Brønsted and Lewis acid sites can be obtained. For example, ^{13}C MAS NMR spectroscopy of adsorbed 2-^{13}C-acetone was used to determine the average acid strength,[8] and ^{31}P NMR spectroscopy of adsorbed trimethylphosphine oxide (TMPO) was employed to probe Brønsted acid sites distributions in various solid acid catalysts.[5,7,10] For 2-^{13}C-acetone adsorbed on solid superacid catalysts such as tungstophosphoric acid ($H_3PW_{12}O_{40}$), the resultant ^{13}C spectrum normally reveals a sharp resonance with a chemical shift greater than 246 ppm,[8] which was taken as a measure of superacidity. Owing to the relatively weak basic nature of acetone (proton affinity or PA value of ca. 194.3 kcal/mol) and the weaker interaction with the acid site compared to that of TMPO (PA = 217.6 kcal/mol), acetone can undergo fast exchange with many Brønsted acidic protons at different acid sites on the experimental NMR time scale, thus usually leading to the observation of an average ^{13}C chemical shift. Hence, ^{13}C MAS NMR spectroscopy of adsorbed acetone can be used to detect only the *overall average* acidity of solid acid catalysts rather than the subtle differences in acid strengths and concentrations. Nevertheless, it is well-

* Corresponding authors. E-mail: dengf@wipm.ac.cn (F.D.), sbliu@sinica.edu.tw (S.-B.L.). Fax: +86-27-87199291 (F.D.), +886-2-23620200 (S.-B.L.).
† The Chinese Academy of Sciences.
‡ Academia Sinica.
§ Xiamen University.

10.1021/jp709739v CCC: $40.75
Published on Web 03/22/2008

known that the acid sites present in zeolites and other solid acid catalysts are normally inhomogeneously distributed. However, because phosphine oxides, such as TMPO, are more basic than acetone and because the ^{31}P nucleus has a wider chemical shift range (ca. 650 ppm) than ^{13}C (ca. 300 ppm), phosphine oxides present several recognizable advantages for acidity characterization in terms of resolving variations in acid strength and concentration. Extensive investigations[7,9,10] have been made using TMPO as the probe molecule for acidity characterization of various solid acid catalysts by solid-state ^{31}P MAS NMR spectroscopy. Accordingly, two types of Brønsted acid sites at supercages and sodalite cages with ^{31}P NMR chemical shifts of 55 and 65 ppm, respectively, have been identified for TMPO adsorbed on faujasite-type zeolites.[7] In addition, up to five different Brønsted acid sites at 86, 75, 67, 63, and 53 ppm have been observed for H-ZSM-5 zeolite.[9a] Moreover, by combining the ^{31}P NMR spectra of adsorbed TMPO with DFT theoretical calculations, an inhomogeneous distribution of Brønsted acid protons in H-MCM-22 zeolite, mostly residing at intracrystalline supercages and extracrystalline side pockets rather than in the sinusoidal channels, has also been observed.[9c,9e]

Although it is well-accepted that the acid strength of solid acids should increase with increasing ^{31}P chemical shift, there is no quantitative measure for the threshold of the ^{31}P chemical shift for superacidity. This, in turn, makes relative comparisons of acid strength based on the ^{31}P chemical shifts of the adsorbed TMPO alone ambiguous. Density functional theory (DFT) quantum chemical calculations thus offer a new opportunity to reveal such correlations from the predicted chemical shifts based on optimized adsorption structure models. In this contribution, systematic DFT calculations have been made for zeolites to predict the adsorption structures and calculate the ^{31}P chemical shifts of TMPO adsorbed on acid sites with varying acid strengths. As a result, a correlation between the ^{31}P chemical shift and the proton affinity (PA) of the Brønsted acid sites can be derived by which a threshold of ^{31}P chemical shift for superacidity can also be determined.

It is well-known that ^{31}P NMR parameters are rather difficult to predict accurately by most theoretical methods. Gee and coworkers[11] calculated the ^{31}P chemical shifts of tetramethyldiphosphine disulfide (TMPS) by the Hartree−Fock (HF) method with different basis sets. Using the 6-311G** basis set, their HF-GIAO results for the ^{31}P chemical shifts were found to be overshielded (toward lower chemical shift values) by about 53 ppm compared to the experimental data. By increasing the size of the basis set to 6-311++G(3df,3pd), the authors were able to obtain a better theoretical result; however, the ^{31}P chemical shift values were still underestimated by about 24 ppm.[11]

It might be inevitable that adequate basis sets and sufficient treatment of electron correlations are needed when predicting reliable NMR parameters. In this context, the GIAO-MP2 (second-order Møller−Plesset perturbation) method has proven to have superior performance for NMR chemical shift predictions.[12] Unfortunately, because GIAO-MP2 normally requires more extensive calculation time and disk space during DFT calculations than the conventional GIAO-HF approach with the same basis sets, the MP2 method is mostly limited to smaller systems.[12d,e,13] Haw et al.[13] revealed a strong correlation between the values calculated by GIAO-HF and GIAO-MP2 for acetone carbonyl ^{13}C isotropic chemical shifts, as demonstrated for a series of complexes between acetone and (Brønsted and Lewis) acid sites. Accordingly, several successful attempts have been made to predict more reliable NMR chemical shifts for larger systems at the GIAO-MP2 level by linear regression based on the GIAO-HF values.[13] Likewise, we were able to obtain a linear correlation for the ^{31}P chemical shifts of TMPO adsorbed on Brønsted acid sites with varying acid strengths by using the 8T cluster model (see below).

An additional objective of this work was to investigate the effects of zeolite pore structures on TMPO adsorption states and their corresponding ^{31}P chemical shifts. This, in turn, allowed us to explore the nature of superacidity in typical zeolites such as H-ZSM-5 by using much larger extended clusters, namely, 26T, 38T, 54T, 58T, and 72T models, to represent different zeolite pore structures. Consequently, accurate predictions of the GIAO-MP2 chemical shifts of TMPO adsorbed on the acid sites of various zeolitic systems can be made through the GIAO-HF values by linear regression.

2. Computational Methods

Because it is a practical shape-selective catalyst, ZSM-5 has been widely utilized for the production of aromatics from light hydrocarbons.[14] Two types of 10-membered-ring (10-MR) pore channels are known to exist in ZSM-5 zeolite: straight, elliptical channels with cross-sectional dimensions of ca. 5.5 × 5.1 Å and sinusoidal (or zigzag) channels with cross-sectional dimensions of ca. 5.6 × 5.4 Å. This unique three-dimensional pore structure allows for reactant and product molecules to diffuse freely during catalytic reactions. In the present study, we used 8T ZSM-5 clusters with different terminal Si−H bond lengths to represent various acid strengths in the solid acid catalyst.[15] A similar method was employed in our previous study on ^{1}H chemical shift calculations of pyridinium-d_5 ions adsorbed on zeolites.[12e]

To exploit the correlation between ^{31}P chemical shift and proton affinity, zeolite H-ZSM-5 was modeled by an 8T [$(H_3SiO)_3$−Si−OH−Al−$(SiOH_3)_3$] cluster in which the Al12−O24(H)−Si12 subgroups were used to represent the Brønsted (Al−OH−Si bridging hydroxyls) acid sites, as shown in Figure 1. These sites were chosen because they are the most likely sites for Al substitution and, being located at the intersections of the straight and zigzag channels of ZSM-5, they are readily accessible to the adsorbents.[16] This was done by performing a partial optimization in which the O_3−Si−OH−Al−O_3 cluster was allowed to relax while the angles of the H_3 groups on the peripheral Si atoms were kept fixed such that they were aligned with the axes connecting Si to the neighboring atoms, thereby mimicking the actual zeolite structure based on crystallographic data. In this way, the integrity of the unique ZSM-5 zeolite structure can then be retained upon optimization of the cluster.[17] None of the atoms in the adsorbed molecules were constrained throughout the configuration optimization of the adsorption complexes. The structural parameters of ZSM-5 used during the calculations were adopted from the available crystallographic data.[18] During calculations, it was assumed that all of the terminal (Si−H) hydrogen atoms in the clusters were located at a distance of r (in angstroms) from the corresponding silicons, with each individual bond oriented along the bond direction to the neighboring oxygen atom. To investigate the correlation between the ^{31}P chemical shift of adsorbed TMPO and the Brønsted acid strength of the solid acid catalyst, a series of different r values (viz., 1.30, 1.40, 1.50, 1.60, 1.75, 2.00, 2.25, 2.50, and 2.75 Å) were used to represent variations in the acid strength (from weak to strong to superacidic).[15] Furthermore, based on information obtained from our previous works,[9c,17] a Si−H bond length of 1.47 Å was employed during calculations to represent acid zeolites. This approach also facilitates a fair comparison between the theoretical and experimental results.

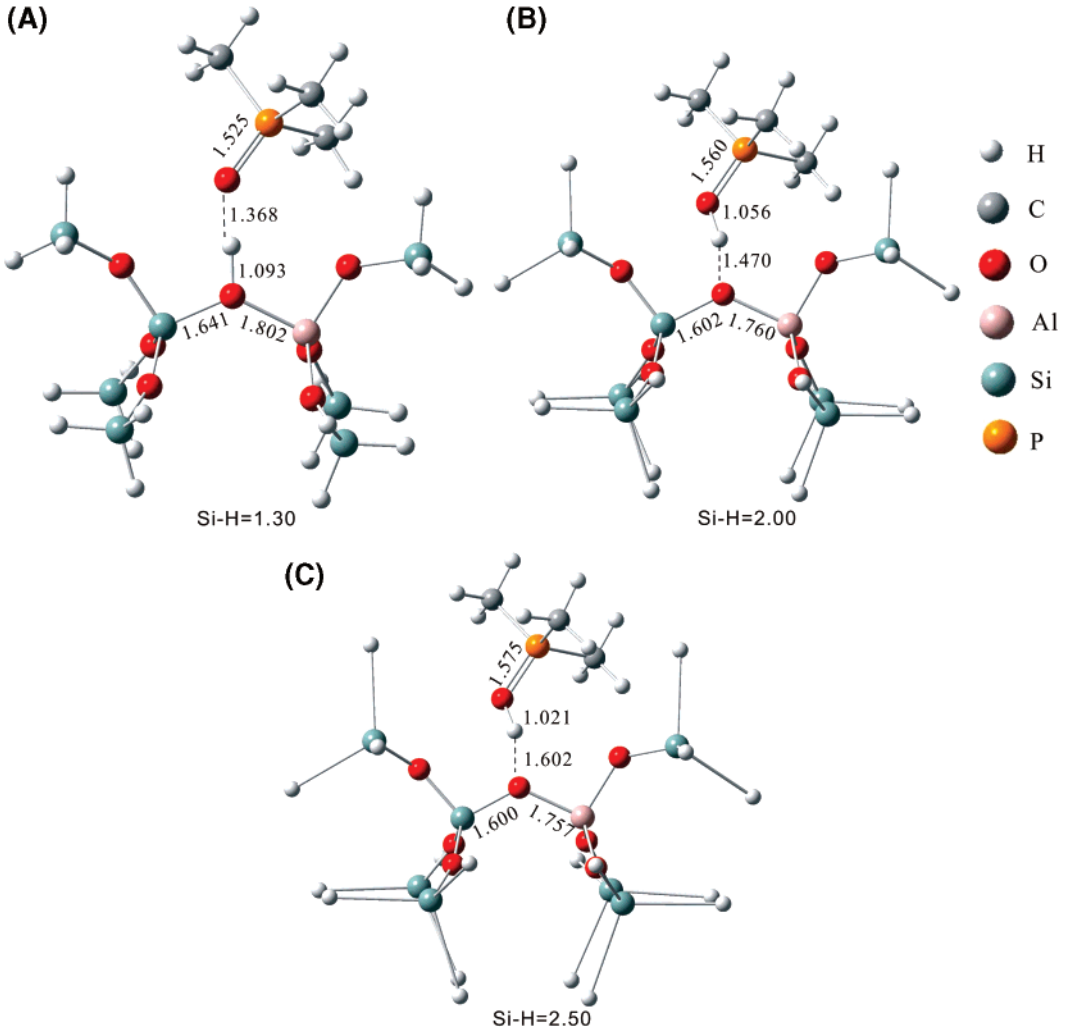

Figure 1. Optimized equilibrium configurations of TMPO adsorbed on the 8T models with Si—H bond lengths of (A) 1.30, (B) 2.00, and (C) 2.50 Å. Selected interatomic distances (in Å) are indicated.

To reveal the range of ^{31}P chemical shifts that can span over acid sites with varying acid strengths in solid acid catalysts, the adsorption configuration and ^{31}P chemical shift of TMPO on the carborane acid H($CHB_{11}Cl_{11}$) were also determined. Carborane acids are protonic acids with well-known "strong yet gentle" properties that facilitate isolation of a wide variety of reactive cations, such as HC_{60}^+, $C_6H_7^+$, *t*-butyl cation, H_3O^+, and H_5O^+.[19,20] In addition, heteropolyoxometalates (HPOMs) have attracted great attention because of their strong acidity and redox properties, and hence, they represent potential practical industrial catalysts for homogeneous and heterogeneous catalyses.[21,22] Our previous ^{13}C MAS NMR studies on acetone adsorbed in tungstophosphoric acid ($H_3PW_{12}O_{40}$) catalyst revealed the appearance of two distinct downfield signals with ^{13}C chemical shifts of 235 and 246 ppm; the latter resonance was attributed to superacidity by comparison with a study of acetone adsorbed in dehydrated catalyst.[8c]

Presumably, by optimizing the adsorption states of the TMPO probe molecule, we should also be able to calculate the ^{31}P chemical shifts of TMPO adsorbed on various solid acid catalysts, such as zeolites, carborane acids, and heteropolyoxometalates, by means of the aforementioned calculation methods. Therefore, the structures of the 8T zeolite models, carborane acid, and $H_3PW_{12}O_{40}$ were optimized with the DMol3 program,[24] using a PW91 density function and the DNP basis set[25] [i.e., a double numerical basis function with polarization functions comparable to the Gaussian basis set 6-31G(d,p)].[26] The adsorption structures of TMPO on the Brønsted acid sites were calculated at the same level. Subsequently, the ^{31}P NMR chemical shift parameters were calculated using the gauge including atomic orbital (GIAO) approach[27] at both the HF/TZVP and MP2/TZVP[28] levels for TMPO adsorbed on 8T cluster models and carborane acid. Using the experimental ^{31}P NMR chemical shift data as benchmarks, the ^{31}P isotropic chemical shifts of the TMPO adsorption complexes were calculated with the HF and MP2 methods at the TZVP level and referenced to the value for physisorbed TMPO (41 ppm).[7,10] As a result, the corresponding calculated absolute chemical shifts were 361.1 and 346.5 ppm at the HF/TZVP and MP2/TZVP levels, respectively. To explore the effects of the zeolite framework on the ^{31}P chemical shift, we also optimized the TMPO adsorption structures on model zeolite ZSM-5 represented by much larger clusters (i.e., 26T, 38T, 54T, 58T, and 72T models) at the PW91/DPN level and predicted the ^{31}P chemical shifts at the GIAO-HF/TZVP level. Using the correlations between the GIAO-HF and GIAO-MP2 results, we could then obtain the theoretical ^{31}P chemical shifts accurately. All of the aforementioned NMR calculations were performed by the Gaussian 03 package.[29]

3. Results and Discussion

3.1. Brønsted Acid Strength of Model Clusters. As shown in Table 1, the bridging O—H bond length, which serves as a

TABLE 1: Proton Affinities (PA, kcal/mol), O−H Bond Lengths (r_{O-H}, Å) of the Bare Zeolites and Assorted Bond Lengths (Å), and Binding Energies (kcal/mol) of the TMPO Adsorption Complexes Predicted on the 8T Cluster with Si−H Bond Lengths (r_{Si-H}) Ranging from 1.30 to 2.75 Å

	bare zeolite		TMPO adsorption structure			
r_{Si-H}	$r_{(O-H)}$	PA	r_{Oz-H}[a]	$r_{P=O}$	r_{H-O}[b]	ΔE_{ads}
1.30	0.974	316.5	1.093	1.525	1.368	8.9
1.40	0.974	301.7	1.136	1.529	1.305	20.2
1.47	0.974	297.9	1.281	1.549	1.151	22.5
1.50	0.974	296.2	1.283	1.549	1.149	23.1
1.60	0.975	290.8	1.351	1.555	1.103	25.0
1.75	0.975	282.2	1.399	1.560	1.077	26.6
2.00	0.976	269.2	1.470	1.560	1.056	33.8
2.25	0.977	258.0	1.529	1.568	1.037	37.2
2.35	0.978	251.2	1.580	1.573	1.027	39.2
2.50	0.978	249.7	1.602	1.575	1.021	41.5
2.75	0.978	243.7	1.642	1.579	1.014	43.6

[a] r_{Oz-H} = bond length between the acidic proton and the zeolite framework oxygen atom. [b] r_{H-O} = bond length between the H and O atoms in the $TMPOH^+$ ions.

parameter for the Brønsted acid strength, increases slightly from 0.974 to 0.978 Å as the Si−H bond length is increased from 1.30 to 2.75 Å. This indicates that the Brønsted acid strength can be modulated theoretically by varying the peripheral Si−H bond lengths of the 8T cluster model.[15] Because there is no definitive scale for the evaluation of acid strength in solid acid catalysts and because the equivalent and commonly used pKa or Hammett acidity values almost always led to an overestimate of acid strength,[30] we define herein the intrinsic acid strengths as the corresponding proton affinity (PA) values observed for the solid acid catalysts. The PA values can be obtained from the energy differences between protonated (Z−OH) and deprotonated ($Z-O^-$) zeolite models[8] and, hence, can be adopted as suitable criteria for the evaluation of intrinsic acid strengths. Haw et al.[8,31,32] previously compared the intrinsic acid strengths for a series of solid acids (e.g., zeolites, $AlCl_3/SiO_2$, SO_3/SiO_2) using the PA values. A smaller PA value represents a Brønsted acid site with a more deprotonated nature and thus a higher acid strength. A Si−H bond length in the range of 1.47−1.50 Å is normally used to represent the zeolite structure during theoretical calculations,[9c,17] in this context, the corresponding PA values were found to vary within the range of 296.2−297.9 kcal/mol, which are in good agreement with the experimental values (291−300 kcal/mol) observed for zeolite ZSM-5.[4b] The data in Table 1 show that, as the Si−H bond distance increases from 1.30 to 2.75 Å, the PA value gradually decreases from 316.5 to 243.7 kcal/mol, covering acid strengths from weak to strong to superacidic.

3.2. Adsorption Configurations of TMPO on Brønsted Acid Sites in Model Clusters. When the TMPO molecules are adsorbed on Brønsted acid sites with relatively low acid strengths (r_{Si-H} = 1.30 Å), adsorption complexes are formed through hydrogen-bonding interactions between the bridging hydroxyl proton and the oxygen atom of the P═O bond (Figure 1). Compared to the bare zeolite model, the zeolite−OH bond of tends to elongate from about 0.974 to 1.093 Å in the adsorption complex. Likewise, the P═O bond length is increased to 1.525 Å with an r_{Si-H} value of 1.30 Å, as compared to that of free (gaseous) TMPO, which is ca. 1.500 Å. As the strength of the Brønsted acid sites is increased, the extent of the protonated nature of TMPO is further enhanced, which is also reflected directly by the variations in the P═O and O−H bond lengths of the $TMPOH^+$ complexes (see Table 1). Consequently, with r_{Si-H} = 2.75 Å (representing TMPO adsorbed on a superacidic site), the zeolite−OH bond length increased from about 0.978 Å (bare model) to 1.642 Å while the O−H bond length of $TMPOH^+$ complex decreased to 1.014 Å, indicating nearly complete proton transfer from the zeolite to the TMPO molecule.

TABLE 2: ^{31}P Chemical Shifts of TMPO Adsorption Complexes Predicted at the HF/TZVP and MP2/TZVP Levels on the 8T Cluster with Si−H Bond Length (r_{Si-H}) Ranging from 1.30 to 2.75 Å

	^{31}P chemical shift (ppm)		
r_{Si-H} (Å)	HF[a]	MP2[a]	MP2[b]
1.30	51.9	45.5	48.1
1.40	53.9	51.2	50.7
1.47	64.7	66.2	65.0
1.50	64.9	66.4	65.3
1.60	68.5	70.8	70.1
1.75	70.6	74.2	72.9
2.00	73.3	76.5	76.5
2.25	77.0	81.1	81.4
2.35	79.5	84.2	84.7
2.50	80.6	85.8	86.1
2.75	83.6	88.9	90.1

[a] For MP2/TZVP calculations, ONIOM(MP2/TZVP:B3LYP/TZVP) was used.[9c,12d,18a] $TMPOH^+$ ions were treated as the high layer, and the 8T zeolite framework was treated as the low layer during the ONIOM calculations. [b] MP2 results predicted by linear regression from the correlation between the GIAO-MP2 and the GIAO-HF calculations in eq 1.

In addition to the TMPO structural parameters, the binding energy (ΔE_{ads}) of TMPO adsorption can also be used to evaluate the acid strength of solid acids. The ΔE_{ads} value for TMPO adsorbed on zeolites can be derived from the energy difference between the adsorbed complex system and the sum of the individual fragments

$$\Delta E_{ads} = E_{ZOH} + E_{TMPO} - E_{TMPO-ZOH}$$

where $E_{TMPO-ZOH}$ represents the single-point energy of the optimized TMPO−zeolite complex and E_{ZOH} and E_{TMPO} are the single-point energies of the optimized bare zeolite and TMPO, respectively. As shown in Table 1, as the acid strength is increased (i.e., as r_{Si-H} increases from 1.30 to 2.75 Å), the binding energy increases from 8.9 to 43.6 kcal/mol. For the weak Brønsted acid sites (PA = 316.5 kcal/mol), a binding energy of 8.9 kcal/mol can therefore be used to represent moderate hydrogen-bonding interactions. The extent of protonation by the Brønsted acid has a considerable effect on the TMPO binding energies, which typically fall in the range of 20.2−39.2 kcal/mol. In contrast, for TMPO adsorbed on solid superacids (typically with PA < 250 kcal/mol),[15] binding energies within the range of 41.5−43.6 kcal/mol are anticipated. It is noteworthy that, as the acid strength is increased, the Mulliken charge distribution of the $TMPOH^+$ fragment is also slightly increased. $TMPOH^+$ typically holds a Mulliken charge of about 0.86 |e| when adsorbed on a superacid ($r_{Si-H} \geq 2.5$ Å), which means that the structure and charge distribution of the $TMPOH^+$ ion protonated by solid superacids are rather close to those of complete protonation by liquid superacids (1.0 |e|), in agreement with the structural results discussed above.

3.3. Correlations of ^{31}P Chemical Shifts Predicted by the GIAO-HF and GIAO-MP2 Methods. Both the HF and MP2 methods with TZVP basis sets were used for ^{31}P NMR chemical shift calculations; the results are presented in Table 2. It is well-known that the calculation of NMR parameters largely depends on the quality of the approximation method employed for the Hamiltonian function. From a comparison of the results in Table

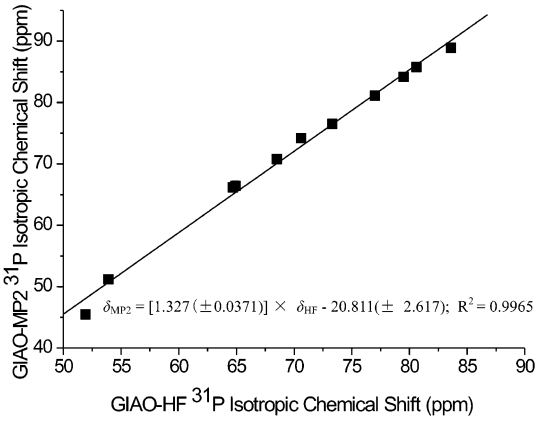

Figure 2. GIAO-MP2/TZVP vs GIAO-RHF/TZVP ^{31}P isotropic chemical shifts of TMPO adsorbed on various Brønsted acid sites with different acid strengths.

2, it is obvious that the electron correlation effects indeed have a notable influence on the calculated ^{31}P chemical shifts. For a hydrogen-bonding system such as the TMPO−zeolite complex with r_{Si-H} = 1.30 Å, the ^{31}P chemical shift predicted by the MP2 method is about 6.4 ppm lower than that predicted by the HF method. In contrast, for the stronger acid sites (1.47 Å < r_{Si-H} < 2.50 Å), the MP2 method predicts ^{31}P resonances that are ca. 2−4 ppm downfield from those predicted by the HF method. It is also noted that the differences between the chemical shifts predicted by the GIAO-HF and GIAO-MP2 methods were even higher (by ca. 5 ppm) for configurations of TMPO adsorbed on superacids ($r_{Si-H} \geq$ 2.5 Å).

Figure 2 displays the correlations between the ^{31}P chemical shifts predicted by the GIAO-MP2 and GIAO-HF methods. Further linear regression of the data shows that the GIAO-MP2 shifts (δ_{MP2}) can be predicted with high accuracy from the GIAO-HF calculations (δ_{HF}) as follows

$$\delta_{MP2} = [1.327\ (\pm 0.0371)] \times \delta_{HF} - 20.811\ (\pm 2.617), \quad R^2 = 0.9965 \quad (1)$$

The high R^2 value indicates an excellent correlation between the chemical shifts predicted by the two methods. Accordingly, this correlation can be used to predict the GIAO-MP2 values of TMPO adsorbed on larger complexes from the calculated GIAO-HF results. As shown in Table 2, the deviations of δ_{MP2} values predicted by linear regression (eq 1) were mostly within 0−1.3 ppm compared to the results directly calculated by the MP2 method for the protonated $TMPOH^+$ models (with $r_{Si-H} \geq$ 1.47 Å). It is noted that the calculated δ_{HF} values indeed differed from the derived δ_{MP2} values by as much as 5 ppm and that the latter represent a more realistic measure for the ^{31}P chemical shifts.

A linear correlation was also found between the ^{31}P chemical shift, δ(MP2, ^{31}P), of protonated $TMPOH^+$ ions ($r_{Si-H} \geq$ 1.47 Å) and the proton affinity (PA, in kcal/mol)

$$\delta(\mathrm{MP2},\ ^{31}\mathrm{P}) = 182.866\ (\pm 5.314) - 0.3902\ (\pm 0.020) \times \mathrm{PA}, \quad R^2 = 0.9913 \quad (2)$$

This linear correlation can thus be used to determine the acid strengths of the solid acids directly from the ^{31}P chemical shifts of adsorbed TMPO (see Figure 3).

In general, a PA value of ca. 250 kcal/mol is considered as the threshold of Brønsted superacidity.[15] As such, it can be inferred that the 8T cluster models exhibit superacid properties when the Si−H bond length exceeds 2.50 Å, in which case a

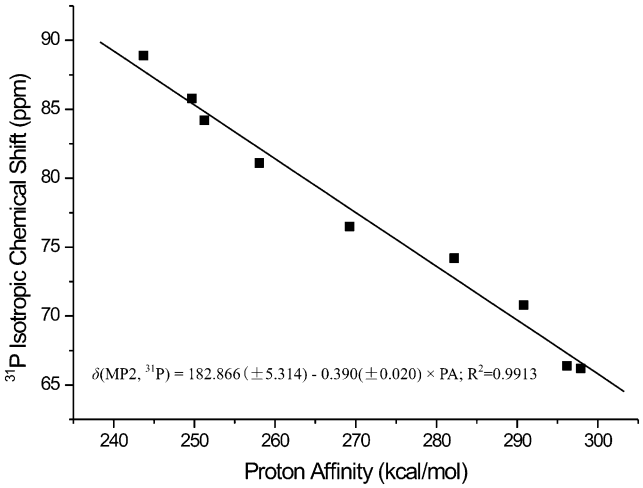

Figure 3. Correlation of the calculated ^{31}P chemical shift of adsorbed $TMPOH^+$ and the proton affinity (PA) of solid acids.

corresponding ^{31}P chemical shift was predicted at 86.1 ppm downfield. Thus, 86 ppm can be considered as the threshold for the ^{31}P chemical shift of TMPO adsorbed on superacid sites in solid acid catalysts such as zeolites and metal oxides.[9] For example, an experimental ^{31}P chemical shift value of 87 ppm was observed for TMPO adsorbed on Brønsted acid sites of sulfated zirconia (SZ) and metal-promoted SZ.[9d] It will be shown later that such a ^{31}P chemical shift threshold for superacidity also prevails for TMPO adsorbed on other types of superacids, such as carborane acid and $H_3PW_{12}O_{40}$. Meanwhile, we also calculated the acetone adsorption configuration on the 8T cluster model with r_{Si-H} values of 2.50 and 2.75 Å. The predicted ^{13}C chemical shifts were found to be 247.1 and 247.4 ppm, respectively.[33] These chemical shift values for superacidity are slightly greater than the previously proposed threshold value (246 ppm) observed experimentally using solid-state ^{13}C MAS NMR spectroscopy of adsorbed 2-^{13}C-acetone.[8,13]

3.4. Configurations and ^{31}P Chemical Shifts of TMPO Adsorbed on Superacids. Figure 4A shows the optimized structure of the bare carborane acid. Owing to the presence of strong hydrogen-bonding interactions, the distances of the acidic proton to the two adjacent chlorinate atoms were found to be 1.416 and 1.888 Å. Accordingly, a PA value of 243.0 kcal/mol was obtained. That the PA value of bare carborane acids is slightly lower than that of the 8T model with an r_{Si-H} value of 2.75 Å (PA = 243.7 kcal/mol; see Table 1) indicates that the former has slightly stronger superacidity. Upon adsorption of TMPO, the P═O bond distance ($r_{P=O}$) was further increased to 1.585 Å, whereas the bond distance (r_{H-O}) between the acidic proton and the oxygen atom of TMPO decreased to 1.007 Å (Figure 4B). From the optimized structure, the calculated ^{31}P chemical shift of the TMPO/carborane acid adsorption complex was found to be 89.6 ppm at the MP2/TZVP level. It is noted that, in comparison to the 8T model (r_{Si-H} = 2.75 Å), whereas a notable increase (ca. 4.8 kcal/mol) in the adsorption energy was obtained for the TMPO/carborane acid adsorption complex, the calculated ^{31}P chemical shift was increased by less than 1 ppm. This indicates that superacidic protons tend to completely protonate the TMPO molecule, leading to a marginal change in the ^{31}P chemical shift. Additional predictions were also made for the ^{13}C chemical shift of adsorbed 2-^{13}C-acetone on carborane acids. In this case, a chemical shift of about 250.7 ppm was obtained, indicating that the carborane acids have a much higher acid strength than $H_3PW_{12}O_{40}$ (246 ppm).[8]

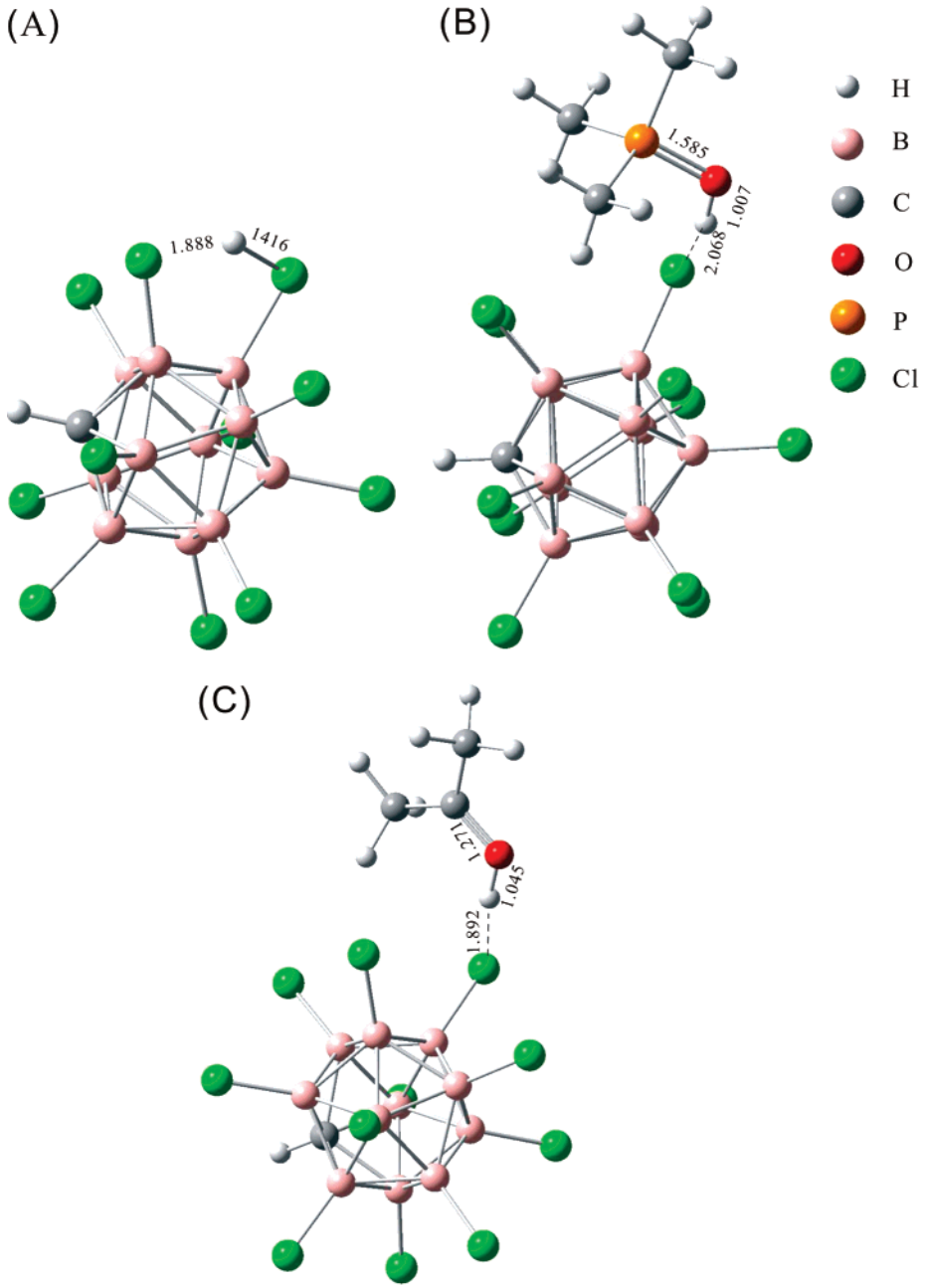

Figure 4. Optimized equilibrium configurations of (A) carborane acids and the corresponding models for (B) TMPO and (C) acetone adsorbed on the protonic acid sites. Selected interatomic distances (in Å) are indicated.

Likewise, we also studied the configuration and ^{31}P chemical shift of TMPO adsorbed on $H_3PW_{12}O_{40}$, which contains three types of oxygen atoms, viz., central (O_a), bridging, and terminal (O_d) oxygens, in the Keggin structure. The bridging oxygen atoms can be further classified into corner-sharing (O_b) and edge-sharing (O_c) oxygen atoms.[21−23] In a recent study using solid-state ^{13}C NMR spectroscopy of 2-^{13}C-acetone adsorbed on $H_3PW_{12}O_{40}$, we demonstrated that the acidic protons are localized on both bridging (O_c) and terminal (O_d) oxygen atoms of the Keggin unit.[8c] Therefore, we proceeded to optimize the adsorption configurations of TMPO on O_c- and O_d-site protons, as shown in Figure 5. Upon adsorption of TMPO onto the O_c and O_d protons, the corresponding P═O bond lengths were found to increase to 1.572 and 1.575 Å, respectively. Together with the observed H−O bond lengths of the $TMPOH^+$ ions, we can thus reach the conclusion that the O_d protons have a higher acid strength than the O_c protons. A similar trend for acid strength was also found for the adsorption of H_2O by Janik and co-workers.[34] For systems containing heavy elements, such as $H_3PW_{12}O_{40}$ (12 tungsten atoms), it is difficult to accurately predict the absolute ^{31}P chemical shifts of adsorption complexes because of the stronger relativistic effects.[35] By comparison with the P═O bond length of the 8T cluster model, we deduced that the ^{31}P chemical shifts for TMPO adsorbed on protons at the O_c and O_d sites were about 83 and 86 ppm, respectively. Thus, this indicates that the protons located at O_d are the superacid sites, whereas those located at O_c can be categorized only as strong Brønsted acid sites.

3.5. Configurations and ^{31}P Chemical Shifts of TMPO Adsorbed on ZSM-5 Zeolite. It is envisaged that, because of strong guest/host interactions, the basic properties of the adsorbed guests will be enhanced upon introduction of basic probe molecules onto microporous zeolites.[36,37] Thus, further studies on the effects of zeolite framework structure on the acid

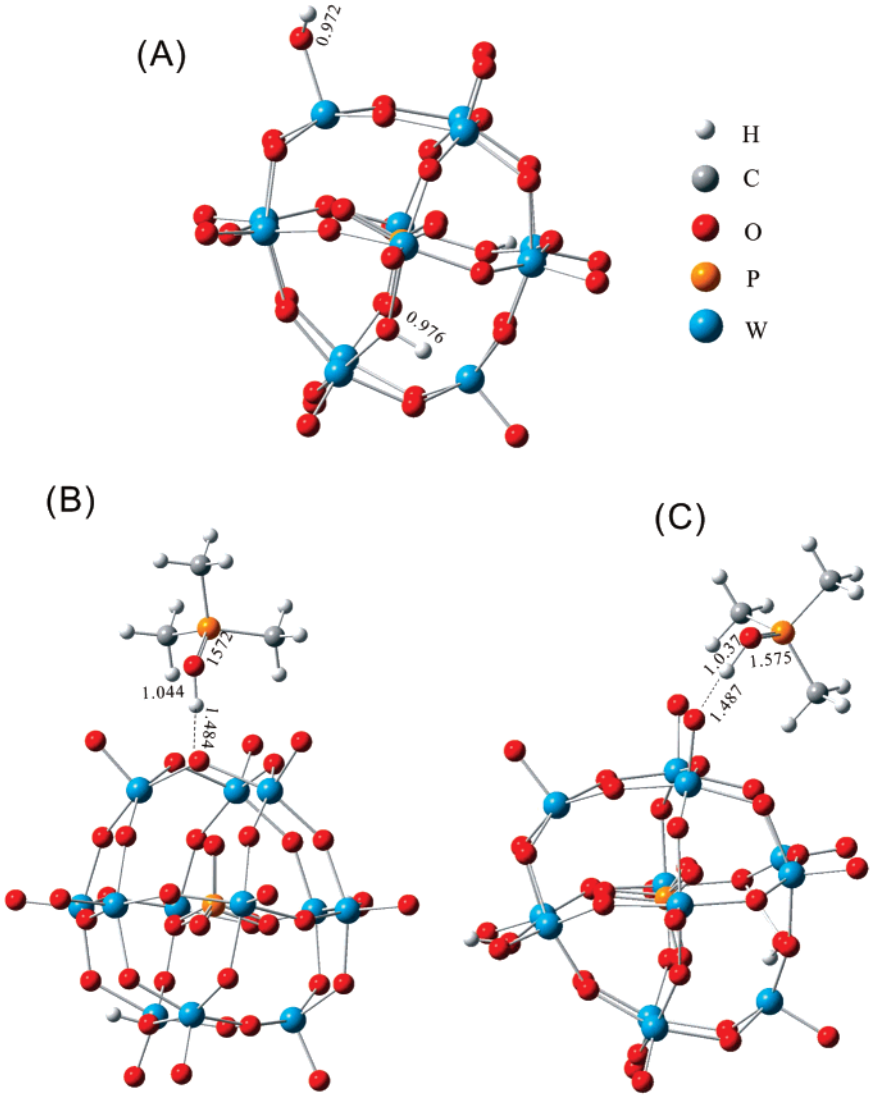

Figure 5. Optimized equilibrium configurations of (A) $H_3PW_{12}O_{40}$ and the corresponding models for TMPO adsorbed on the (B) O_c and (C) O_d protonic acid sites. Selected interatomic distances (in Å) are indicated.

properties and TMPO adsorption structure are needed. Therefore, we extended the 8T cluster model to a series of larger cluster models (26T, 38T, 54T, 58T, and 72T) with r_{Si-H} at 1.47 Å. The use of larger cluster models facilitates investigation of long-range electrostatic effects from the Madelung potential of the zeolite framework, which is quite pronounced for ZSM-5 (with a channel diameter of ca. 0.55 nm, comparable to the molecular size of TMPO, which has a kinetic diameter of 0.55 nm).[14] As shown in Table 3, the PA values remain almost unchanged (280−283 kcal/mol) as the cluster size is increased, indicating that, although the intrinsic acidity of the zeolite increases with increasing degree of framework extension, the acid strength is still lower than that of superacids (typically with a PA threshold of 250 kcal/mol).

The optimized equilibrium configurations of TMPO adsorbed on various cluster models are shown in Figures 6 and 7. Because the Brønsted acid sites are known to be located at the intersections of the straight and sinusoidal channels of zeolite ZSM-5, we extended the pore structure from both the [100] and [010] faces of the structural frameworks. As we extended along the [100] face of zeolite ZSM-5, the P═O bond lengths were found to gradually increase from 1.549 Å in the 8T cluster to 1.553 Å (26T), 1.554 Å (38T), 1.562 Å (52T), 1.571 Å (58T), and 1.576 Å (72T) (see Table 3). Meanwhile, the O—H bond lengths gradually decreased from 1.151 Å (8T) to 1.122 Å (26T), 1.111 Å (38T), 1.064 Å (52T), 1.045 Å (58T), and 1.031 Å (72T). Note that the P═O and O—H bond lengths observed for the 72T cluster model were extracted along the [010] pore face. In any case, it is clear that, as the cluster size of the zeolite framework is extended, the degree of protonation for TMPO

TABLE 3: Proton Affinities (PA, kcal/mol), Assorted Bond Lengths (Å), and ^{31}P Chemical Shifts (ppm) of TMPO Adsorbed on a Series of Extended Zeolite Structures from 8T to 72T Cluster Models

cluster model	PA	TMPO adsorption structure			chemical shift	
		r_{Oz-H}[a]	$r_{P=O}$[b]	r_{H-O}	HF	MP2[c]
8T	297.9	1.281	1.549	1.151	64.7	65.0
26T	281.2	1.327	1.553	1.122	68.7	70.4
38T	280.9	1.354	1.554	1.111	69.2	71.0
52T	280.3	1.443	1.562	1.064	74.4	77.9
58T	282.8	1.516	1.571	1.045	76.1	80.2
72T	281.0	1.587	1.576	1.031	81.0	86.7

[a] r_{Oz-H} = bond length between the acidic proton and zeolite framework oxygen atom. [b] r_{H-O} = bond length between the H and O atoms in the $TMPOH^+$ ions. [c] MP2 results predicted by linear regression between the GIAO-MP2 and the GIAO-HF calculations in eq 1.

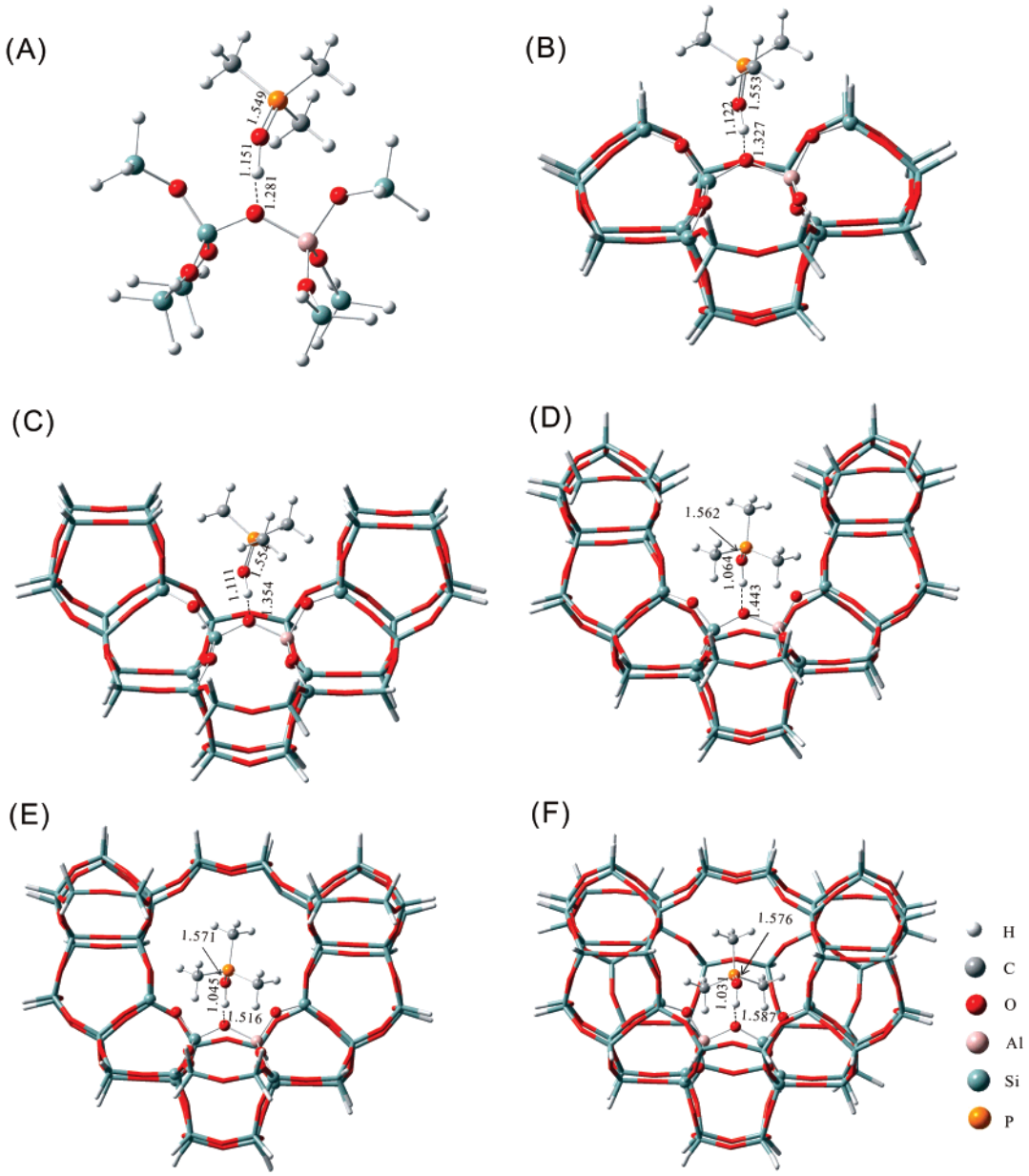

Figure 6. Optimized equilibrium configurations of TMPO adsorbed on the (A) 8T, (B) 26T, (C) 38T, (D) 52T, (E) 58T, and (F) 72T models viewed along the [100] face of the ZSM-5 framework. Selected interatomic distances (in Å) are indicated.

increases, leading to an increasing stabilization of the $TMPOH^+$ complexes. Other than that, no simple correlations in the P═O and O—H bond lengths with cluster size can be inferred.

To justify the appropriateness of predicting ^{31}P chemical shifts of TMPO adsorbed on extended zeolite cluster models based on the correlation derived from HF and MP2 calculation results of the simplified 8T model (vide supra), additional MP2-level calculation were performed based on the 26T model. Accordingly, a theoretical value of 69.8 ppm was obtained for the ^{31}P chemical shift of adsorbed TMPO, in excellent agreement with the value (70.4 ppm) predicted using the HF vs MP2 correlation in eq 1. It is worth pointing out that a similar procedure was employed by Haw and co-workers[13] to predict the ^{13}C chemical shifts of acetone complexes in larger (8T) zeolite ZSM-5 cluster model based on an HF—MP2 correlation derived from calculation results of acetone interacting with a variety of different molecules, such as HCl, CH_3OH, H_2F_2, HF, BF_3, AlF_3, and $AlCl_3$. Thus, in view of the fact that MP2-level calculations are not readily practical for larger cluster models (exceeding 26T) because of the limitations and powers of computing facilities, it seems justifiable to adopt the HF vs MP2 correlation (based on 8T model) for the prediction of ^{31}P chemical shifts of TMPO adsorbed on larger zeolite cluster models (Table 3).

As a result, a monotonic downfield shift of the ^{31}P chemical shift was observed, following the trend 65.0 ppm (8T), 70.4 ppm (26T), 71.0 ppm (38T), 77.9 ppm (52T), 80.2 ppm (58T), and 86.7 ppm (72T). Except for the gradual increase in ^{31}P chemical shift with cluster size, no obvious correlation between the values can be deduced. That the strong Brønsted acid sites give rise to a downfield chemical shift of 86 ppm for TMPO adsorbed on H-ZSM-5 zeolites is in good agreement with previous experimental studies.[9a,9b] This indicates that the acidity induced in the presence of TMPO is much different from the intrinsic acidity of the parent zeolites.[36,37] Clearly, the interactions between the adsorbed TMPO probe molecule and zeolite framework are responsible for the increases in the calculated ^{31}P chemical shifts. Thus, taking the microporous structure of zeolite into account, the introduction of TMPO tends to induce Brønsted acid protons with acid strengths similar to those observed for superacids.

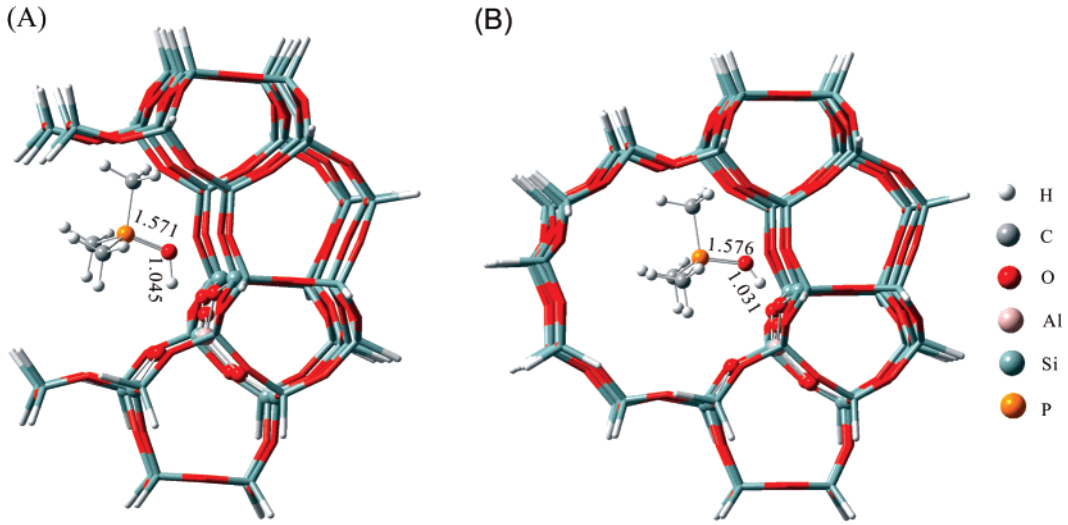

Figure 7. Optimized equilibrium configurations of TMPO adsorbed on the (A) 58T and (B) 72T models viewed along [010] face of the ZSM-5 framework. Selected interatomic distances (in Å) are indicated.

There has been a controversial debate in the past on whether zeolites exhibit superacidity. In the case of a solid-state ^{13}C MAS NMR study using adsorbed 2-^{13}C-acetone as the probe molecule, a ^{13}C chemical shift of 223 ppm was observed for H-ZSM-5.[8a,8b] By comparison, the ^{13}C chemical shift observed for solid superacid HPW was ca. 246 ppm,[8c] suggesting that zeolites could be classified only as solid acid catalysts with moderate to high acid strengths,[8a,8b] which is also in good agreement with our calculated PA values for ZSM-5. In this case, the adsorbed acetone molecules can do fast exchange among different Brønsted acid sites within the NMR time scale; thus, usually only an average chemical shift (i.e., acid strength) can be observed. More specifically, acidity characterization by means of ^{13}C MAS NMR spectroscopy of adsorbed acetone result in only a single resonance representing the *overall* average acid strength, in turn leading to a faulty conclusion that ZSM-5 zeolites contain Brønsted acid sites with only moderate to high acid strengths. In this context, ^{31}P MAS NMR spectroscopy of adsorbed trialkylphosphine oxides (such as TMPO) as probes represents a superior technique for acidity characterization. In the case of 10-membered-ring zeolites such as ZSM-5, TMPO (having the appropriate kinetic diameter) appears to be the most preferable candidate as the probe molecule.[9a] This is due to the fact that it is capable of probing not only the type (Brønsted vs Lewis) and concentration (amount) but also the distribution of acid sites with different acid strengths.[9] For example, up to five ^{31}P resonance peaks at 86, 75, 67, 63, and 53 ppm were observed[9a] for H-ZSM-5 (Si/Al = 15) using TMPO as the probe molecule. The occurrence of these resonance peaks was ascribed to acidic protons located at different T sites.[9a] Obviously, there is a distribution of acid sites with varying acid strengths in H-ZSM-5 zeolite, ranging from weak to strong to superacidic. We also concluded that, following the descending order of acid strength, the relative concentrations of the resonances at 86, 75, 67, 63, and 53 ppm were 0.5%, 22.4%, 37.5%, 36.6%, and 3.0%, respectively.[9a] Furthermore, as the Si/Al ratio of the H-ZSM-5 zeolite is increased, a notable increase in the relative concentration of the 86 ppm resonance (at the expense of sites with lower acid strengths) was observed. Similar observations have also been made for other types of zeolites, such as HMCM-22 (Si/Al = 13) and H-mordenite (Si/Al =10), in which the ^{31}P chemical shifts (and relative concentrations) observed for acid sites with the highest acid strength were found to be 84.6 ppm (4.3%) and 87.7 ppm (2.2%), respectively.[9b,9e] This experimental evidence together with the results obtained from the present theoretical study thus lead us to the conclusion that, although the amount of superacid sites depends on the Si/Al ratio of the zeolites, typically more than 95% of the acid sites have acid strengths in the range of weak to strong acidity and only less than 5% of Brønsted acidity can be categorized as superacidic. In addition to the concentration and distribution of acid sites, which are crucial for catalytic activity during heterogeneous hydrocarbon conversions, the structure and physical properties of solid acid catalysts also play important roles, especially for shape-selective catalytic reactions. The theoretical predictions of the ^{31}P chemical shift threshold of TMPO reported herein therefore should not only provide new insight toward understanding of the reaction mechanism involved during acid catalysis but also offer new opportunities for the design and/or modification of solid acid catalysts for practical industrial applications. Further theoretical studies on various zeolites with different structures and pore sizes and for TMPO adsorbed on different T sites of zeolites such as H-ZSM-5 are being undertaken.

4. Conclusions

The TMPO adsorption structures and the corresponding ^{31}P NMR chemical shifts have been predicted theoretically based on an 8T cluster model with varying Si—H bond lengths to evaluate Brønsted acid sites having different acid strengths (from weak to strong to superacidic) in zeolitic catalysts. Correlations between the ^{31}P chemical shifts and proton affinities of the solid acid were also derived. Accordingly, a threshold of 86 ppm for the ^{31}P chemical shift of TMPO adsorbed on superacid sites in zeolites has been determined. Further extension of the zeolite ZSM-5 model structure cluster size from 8T to 72T revealed that the adsorption states of $TMPOH^+$ complexes become increasingly more stable, eventually leading to acid sites with ultrahigh acid strengths similar to those of solid superacids.

Acknowledgment. This work was supported by the National Natural Science Foundation of China (20703058, 20425311, 20673139, and 20425312) and by the National Science Council (NSC95-2113-M-001-040-MY3), Taiwan. We thank Shanghai Supercomputer Center (SSC) of China for technical support. A.M.Z. thanks NSC and IAMS, Academia Sinica, for the visiting research fellowship, and S.B.L. is grateful for the visiting professorship from WIPM, Chinese Academy of Sciences.

References and Notes

(1) (a) Matsuhashi, H.; Tanaka, T.; Arata, K. *J. Phys. Chem. B* **2001**, *105*, 9669. (b) Sulikowski, B.; Datka, J.; Gil, B.; Ptaszynski, J.; Klinowski, J. *J. Phys. Chem. B* **1997**, *101*, 6929.

(2) (a) Lee, C.; Parrillo, D. J.; Gorte, R. J.; Farneth, W. E. *J. Am. Chem. Soc.* **1996**, *118*, 3262. (b) Niwa, M.; Suzuki, K.; Isamoto, K.; Katada, N. *J. Phys. Chem. B* **2006**, *110*, 264. (c) Brand, H. V.; Curtiss, L. A.; Iton, L. E. *J. Phys. Chem.* **1993**, *97*, 12773.

(3) Kotrla, J.; Kubelkova, L.; Lee, C. C.; Gorte, R. J. *J. Phys. Chem. B* **1998**, *102*, 1437.

(4) Kresnawahjuesa, O.; Kuhl, G. H.; Gorte, R. J.; Quierini, C. A. *J. Catal.* **2002**, *210*, 106.

(5) Peng, L.; Chupas, P. J.; Grey, C. P. *J. Am. Chem. Soc.* **2004**, *126*, 12254.

(6) Ma, D.; Deng, F.; Fu, R.; Han, X.; Bao, X. *J. Phys. Chem. B* **2001**, *105*, 1770.

(7) Karra, M. D.; Sutovich, K. J.; Mueller, K. T. *J. Am. Chem. Soc.* **2002**, *124*, 902.

(8) (a) Haw, J. F.; Xu, T.; Nicholas, J. B.; Gorgune, P. W. *Nature* **1997**, *389*, 832. (b) Haw, J. F.; Nicholas, J. B.; Xu, T.; Beck, L. W.; Ferguson, D. B. *Acc. Chem. Res.* **1996**, *29*, 259. (c) Yang, J.; Janik, M. J.; Ma, D.; Zheng, A.; Zhang, M.; Neurock, M.; Davis, R. J.; Ye, C.; Deng, F. *J. Am. Chem. Soc.* **2005**, *127*, 18274.

(9) (a) Zhao, Q.; Chen, W. H.; Huang, S. J.; Wu, Y. C.; Lee, H. K.; Liu, S. B. *J. Phys. Chem. B* **2002**, *106*, 4462. (b) Zhao, Q.; Chen, W. H.; Huang, S. J.; Liu, S. B. *Stud. Surf. Sci. Catal.* **2003**, *145*, 205. (c) Zheng, A.; Chen, L.; Yang, J.; Zhang, M.; Su, Y.; Yue, Y.; Ye, C.; Deng, F. *J. Phys. Chem. B* **2005**, *109*, 24273. (d) Chen, W. H.; Ko, H. H.; Sakthivel, A.; Huang, S. J.; Liu, S. H.; Lo, A. Y.; Tsai, T. C.; Liu, S. B. *Catal. Today* **2006**, *116*, 111. (e) Huang, S. J.; Zhao, Q.; Chen, W. H.; Han, X.; Bao, X.; Lo, P. S.; Lee, H. K.; Liu, S. B. *Catal. Today* **2004**, *97*, 25. (f) Huang, S. J.; Tseng, Y. H.; Mou, Y.; Liu, S. B.; Huang, S. H.; Lin, C. P.; Chan, J. C. C. *Solid State Nucl. Magn. Reson.* **2006**, *29*, 272.

(10) (a) Kao, H. C.; Yeh, M. *Microporous Mesoporous Mater.* **2002**, *53*, 1. (b) Rakiewicz, E. F.; Peters, A. W.; Wormsbecher, R. F.; Sutovich, K. J.; Mueller, K. T. *J. Phys. Chem. B* **1998**, *102*, 2890.

(11) Gee, M.; Wasylishen, R. E.; Eichele, K.; Britten, J. F. *J. Phys. Chem. A* **2000**, *104*, 4598.

(12) (a) Sieber, S.; Schleyer, P. V. R.; Gauss, J. *J. Am. Chem. Soc.* **1993**, *115*, 6987. (b) Xu, T.; Torres, P. D.; Barich, D. H.; Nicholas, J. B.; Haw, J. F. *J. Am. Chem. Soc.* **1997**, *119*, 396. (c) Xu, T.; Barich, D. H.; Torres, P. D.; Haw, J. F. *J. Am. Chem. Soc.* **1997**, *119*, 406. (d) Zheng, A.; Yang, M. H.; Yue, Y.; Ye, C.; Deng, F. *Chem. Phys. Lett.* **2004**, *399*, 172. (e) Zheng, A.; Zhang, H.; Chen, L.; Yue, Y.; Ye, C.; Deng, F. *J. Phys. Chem. B* **2007**, *111*, 3085.

(13) Barich, D. H.; Nicholas, J. B.; Xu, T.; Haw, J. F. *J. Am. Chem. Soc.* **1998**, *120*, 12342.

(14) Chen, N. Y.; William R. G.; Frank, G. D. *Shape Selective Catalysis in Industrial Applications, Chemical Industries*; Marcel Dekker Inc.: New York, 1989; p 36.

(15) (a) Kramer, G. J.; Vansanten, R. A.; Emeis, C. A.; Nowak, A. K. *Nature* **1993**, *363*, 529. (b) Zheng, X.; Blowers, P. *J. Mol. Catal. A* **2005**, *229*, 77. (c) Zheng, X.; Blowers, P. *J. Phys. Chem. A* **2005**, *109*, 10734.

(16) (a) Brand, H. V.; Curtiss, L. A.; Iton, L. E. *Phys. Chem.* **1993**, *97*, 7. (b) Pantu, P.; Pabchanda, S.; Limtrakul, J. *Chem. Phys. Chem.* **2004**, *5*, 1901.

(17) Zheng, A.; Chen, L; Yang, J; Yue, Y; Ye, C.; Lu, X; Deng, F. *Chem. Commun.* **2005**, 2474.

(18) van Koningsveld, H.; van Bekkum, H.; Jansen, J. C. *Acta Crystallogr. B* **1987**, *43*, 127.

(19) Stoyanov, E. S.; Hoffmann, S. P.; Juhasz, M.; Reed, C. A. *J. Am. Chem. Soc.* **2006**, *128*, 3160.

(20) Koppel, I. A.; Burk, P.; Koppel, I.; Leito, I.; Sonoda, T.; Mishima, M. *J. Am. Chem. Soc.* **2000**, *122*, 5114.

(21) (a) Baba, T.; Sakai, J.; Ono, Y. *Bull. Chem. Soc. Jpn.* **1982**, *55*, 2657. (b) Baba, T.; Sakai, J.; Watanabe, H.; Ono, Y. *Bull. Chem. Soc. Jpn.* **1982**, *55*, 2555. (c) Baba, T.; Ono, Y. *Appl. Catal.* **1983**, *8*, 315.

(22) Baronetti, G.; Thomas, H.; Querini, C. A. *Appl. Catal. A* **2001**, *217*, 131.

(23) Ono, Y.; Baba, T.; Sakai, J.; Keii, T. *Chem. Commun.* **1981**, 400.

(24) *Dmol3*; Accelrys Inc.: San Diego, CA, 2000.

(25) Perdew, J. P.; Wang, Y. *Phys. Rev. B* **1986**, *33*, 8822.

(26) Hehre, W. J.; Ditchfield, R.; Pople, J. A. *J. Chem. Phys.* **1972**, *56*, 2257.

(27) (a) Wolinski, K.; Hinton, J. F.; Pulay, P. *J. Am. Chem. Soc.* **1990**, *112*, 8251. (b) Ditchfield, R. *Mol. Phys.* **1974**, *27*, 789.

(28) Godbout, N.; Salahub, D. R.; Andzelm, J.; Wimmer, E. *Can. J. Chem.* **1992**, *70*, 560.

(29) Frisch, M. J.; Trucks, G. W.; Schlegel, H. B.; Scuseria, G. E.; Robb, M. A.; Cheeseman, J. R.; Montgomery, J. A., Jr.; Vreven, T.; Kudin, K. N.; Burant, J. C.; Millam, J. M.; Lyengar, S. S.; Tomasi, J.; Barone, V.; Mennucci, B.; Cossi, M.; Scalmani, G.; Rega, N.; Petersson, G. A.; Nakatsuji, H.; Hada, M.; Ehara, M.; Toyota, K.; Fukuda, R.; Hasegawa, J.; Ishida, M.; Nakajima, T.; Honda, Y.; Kitao, O.; Nakai, H.; Klene, M.; Li, X.; Knox, J. E.; Hratchian, H. P.; Cross, J. B.; Adamo, C.; Jaramillo, J.; Gomperts, R.; Stratmann, R. E.; Yazyev, O.; Austin, A. J.; Camml, R.; Pomelli, C.; Ochterski, J. W.; Ayala, P. Y.; Morokuma, K.; Voth, G. A.; Salvador, P.; Dannenberg, J. J.; Zakrzewski, V. G.; Dapprich, S.; Daniels, A. D.; Strain, M. C.; Farkas, O.; Malick, D. K.; Rabuck, A. D.; Raghavachari, K.; Foresman, J. B.; Ortiz, J. V.; Cui, Q.; Baboul, A. G.; Clifford, S.; Cioslowski, J.; Stefanov, B. B.; Liu, G.; Liashenko, A.; Piskorz, P.; Komaromi, I.; Martin, R. L.; Fox, D. J.; Keith, T.; Al-Laham, M. A.; Peng, C. Y.; Nanayakkara, A.; Challacombe, M.; Gill, P. M. W.; Johnson, B.; Chen, W.; Wong, M. W.; Gonzalez, C.; Pople, J. A. *Gaussian 03*, revision B.05; Gaussian, Inc.: Pittsburgh, PA 2003.

(30) Gorte, R. J. *Catal. Lett.* **1999**, *62*, 1.

(31) Xu, T.; Kob, N.; Grago, R. S.; Nicholas, J. B.; Haw, J. F. *J. Am. Chem. Soc.* **1997**, *119*, 12231.

(32) Zhang, J.; Nicholas, J. B.; Haw, J. F. *Angew. Chem.* **2000**, *112*, 3440.

(33) The ^{13}C chemical shifts of the carboxyl carbon on acetone adsorbed on the 8T cluster models with r_{Si-H} at 2.50 and 2.75 Å were predicted by the ONIOM-GIAO method (MP2/TZVP:B3LYP/TZVP).[12d,17] Acetone−H^+ ions were treated as the high layer, and the 8T zeolite framework was treated as the low layer during the ONIOM calculations. The ^{13}C chemical shifts were referenced to the gas-phase protonated acetone ion (260.1 ppm).[12]

(34) Janik, M. J.; Campbell, K. A.; Bardin, B. B.; Davis, R. J.; Neurock, M. *Appl. Catal. A* **2003**, *256*, 51.

(35) Corminboeuf, C. *Chem. Phys. Lett.* **2006**, *418*, 437.

(36) Marquez, F.; Garcia, H.; Palomares, E.; Fernandez, L.; Corma, A. *J. Am. Chem. Soc.* **2000**, *122*, 6520.

(37) Scaiano, J. C.; Garcia, H. *Acc. Chem. Res.* **1999**, *32*, 783.